

Dominant particle-hole contributions to the phonon dynamics in the spinless one-dimensional Holstein model

S. Sykora¹, A. Hubsch², and K. W. Becker¹

¹ Institut für Theoretische Physik, Technische Universität Dresden, 01062 Dresden, Germany

² Max-Planck-Institut für Physik komplexer Systeme, Nothnitzer Straße 38, 01187 Dresden, Germany

PACS. 71.10.Fd { Lattice fermion models (Hubbard model, etc.) .

PACS. 71.30.+h { Metal-insulator transitions and other electronic transitions.

Abstract. { In the spinless Holstein model at half-filling the coupling of electrons to phonons is responsible for a phase transition from a metallic state at small coupling to a Peierls distorted insulated state when the electron-phonon coupling exceeds a critical value. For the adiabatic case of small phonon frequencies, the transition is accompanied by a phonon softening at the Brillouin zone boundary whereas a hardening of the phonon mode occurs in the anti-adiabatic case. The phonon dynamics studied in this letter do not only reveal the expected renormalization of the phonon modes but also show remarkable additional contributions due to electronic particle-hole excitations.

Introduction. { The electron-phonon (EP) interaction leads in many low-dimensional materials like MX chains, conjugated polymers, or organic transfer complexes [1,2] to structural distortions. Thus, Peierls transition and charge-density wave instability have been observed in such systems. Many interesting questions arise not only with respect to the associated metal to insulator transition but also concerning the signatures of the single-particle excitations in the different phases. The interest in models of electrons interacting with phonons has been renewed by intriguing findings which implicate an important role of the EP coupling in a wide range of materials with strong electronic correlations; high-temperature superconductors, manganites, or C₆₀ based compounds are well-known examples [3].

The one-dimensional Holstein model of spinless fermions (HM),

$$H = \sum_{hi,ji} (c_i^\dagger c_j + \text{h.c.}) + \sum_i \omega_0 b_i^\dagger b_i + g \sum_i (b_i^\dagger + b_i) n_i; \quad (1)$$

is the simplest realization of a strongly coupled EP system and considers the local interaction g between the electron density $n_i = c_i^\dagger c_i$ and dispersion-less phonons with frequency ω_0 . The c_i^\dagger (b_i^\dagger) are fermionic (bosonic) creation operators of electrons (phonons), and $\sum_{hi,ji}$ denotes the summation over all neighboring lattice sites i and j . With increasing g , the half-filled HM undergoes a quantum phase transition from a metallic state to a dimerized Peierls phase.

Because the HM is not exactly solvable a number of analytical and numerical methods have been applied (see references in [4]) to study the phase transition. In particular, the properties of the insulating phase have been shown to be sensitive to the relation between band-width and EP coupling [5]: a band insulator is found in the adiabatic case $\lambda_0 = t \ll 1$ whereas a polaronic superlattice occurs in the anti-adiabatic limit $\lambda_0 = t \gg 1$.

Recently, we applied the projector-based renormalization method (PRM) [6] to the HM at half-filling where both the metallic and the insulating case has been studied [4,7]. Here, we extend our work [4] to discuss the phonon as well as the electronic one-particle excitation spectrum in more detail. Most of the work is restricted to the adiabatic limit $\lambda_0 = t \ll 1$ where a phonon softening is found if the EP coupling approaches the critical value g_c of the transition. In contrast, a phonon stiffening occurs for $\lambda_0 = t \gg 1$. The most remarkable findings of our present work are the large contributions to the phonon spectrum which are caused by the coupling to electronic particle-hole excitations. Note that presently in the anti-adiabatic limit the insulating phase can not be studied because no stable solutions are found for $t > g$.

Theoretical approach. We use the recently derived uniform description of metallic and insulating phases of the half-filled HM [4]. This approach employs the PRM [6] where an effective Hamiltonian $\tilde{H} = \lim_{\lambda \rightarrow 0} \lambda H$ is obtained by a sequence of unitary transformations, $H(\lambda) = e^X \lambda H e^{-X}$, by which transitions between eigenstates of the unperturbed part H_0 of the Hamiltonian are eliminated in steps. The respective transition energies are used as renormalization parameter. X has to be adjusted so that $H(\lambda)$ only contains excitations with energies smaller or equal (\leq). In this way, an effectively free model,

$$\tilde{H} = \sum_{k>0}^X \sum_{\mu,\nu} c_{\mu k}^\nu c_{\nu k}^\mu + \sum_{k>0}^X \tilde{c}_{0k}^\nu c_{1k}^\nu + \hbar \omega : + \sum_{q>0}^X b_{-q}^\dagger b_q^\dagger + b_{-1}^\dagger b_1^\dagger + E; \quad (2)$$

was found in Ref. [4] which is used here in order to calculate the phonon spectral function,

$$B(q; \lambda) = \frac{1}{2} \int_{-1}^1 [q(t); \frac{\nu}{q}] e^{i\lambda t} dt \quad (3)$$

and to consider the two electronic one-particle spectral functions

$$A_k^+(\lambda) = \frac{1}{2} \int_{-1}^1 \alpha_k(t) c_k^\nu e^{i\lambda t} dt; \quad A_k(\lambda) = \frac{1}{2} \int_{-1}^1 c_k^\nu \alpha_k(t) e^{i\lambda t} dt; \quad (4)$$

In Eq. (2) a reduced Brillouin zone has been introduced in order to allow a dimerization of the system, and both the fermionic and bosonic one-particle operators as well as the model parameters have additional band indices, $\mu, \nu = 0, 1$. In Eq. (3), $q = b_q + b_q^\dagger$ is proportional to the Fourier transformed lattice displacement. $A_k^+(\lambda)$ describes the creation of an electron with momentum k at time zero and its annihilation at time t whereas in $A_k(\lambda)$ first an electron is annihilated. As is well-known, $A_k(\lambda) [A_k^+(\lambda)]$ can be measured by [inverse] photoemission.

To evaluate Eqs. (3) and (4) within the PRM approach we use that expectation values are invariant with respect to an unitary transformation under the trace. Thus, $B(q; \lambda)$, $A_k^+(\lambda)$, and $A_k(\lambda)$ can easily be computed if the phononic and electronic one-particle operators are transformed in the same way as the Hamiltonian (see Ref. [7] for more details). For instance, by taking the fully transformed phonon operator $\tilde{b}_q^\nu = b_q^\nu + \frac{1}{N} \sum_k \tilde{c}_{kq}^\nu c_{k+q}^\nu$ we

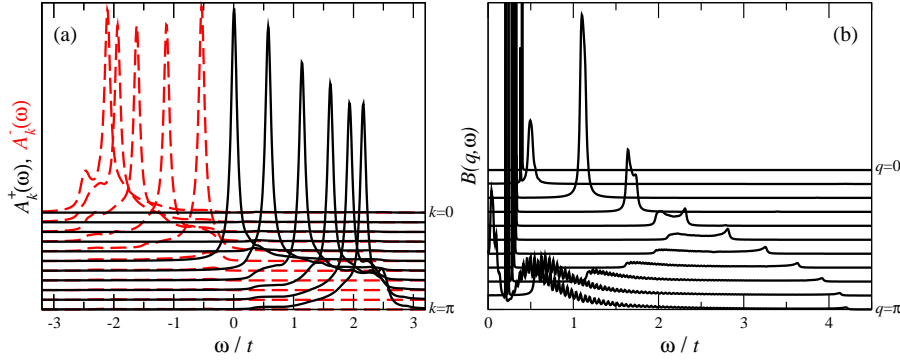


Fig. 1 (Color online) Panel (a) shows the electronic one-particle spectral functions $A_k^+(\omega)$ (solid lines) and $A_k^-(\omega)$ (dashed lines) for the metallic phase in the adiabatic case, $\epsilon_0 = 0.4t$, $g = 0.632t$ where a one-dimensional HM with 500 lattice sites has been considered at half-filling. The Fermi energy is located at $\epsilon = 0$. Panel (b) shows the corresponding one-phonon spectral function $B(q; \omega)$.

obtain for the phonon spectral function in the metallic region

$$B(q; \omega) = \frac{\tilde{f}_q \tilde{f}_q^*}{\epsilon_q} (\epsilon - \epsilon_q) + \frac{\tilde{f}_q \tilde{f}_q^*}{\epsilon_q} (\epsilon + \epsilon_q) + \frac{1}{N} \sum_k \tilde{f}_{k,q} \tilde{f}_{k,q}^* \frac{f(\epsilon_k) - f(\epsilon_{k+q})}{\epsilon_{k+q} - \epsilon_k} (\epsilon_{k+q} - \epsilon_k) \quad (5)$$

where terms with two bosonic creation or annihilation operators have been neglected. The coefficients \tilde{f}_q , \tilde{f}_q^* , and $\tilde{f}_{k,q}$ can be determined within the PRM approach. Eqs. (3) and (4) fulfill sum rules, $\sum_k B(q; \omega) = 1$ and $\sum_k [A_k^+(\omega) + A_k^-(\omega)] = 1$, which are not affected by the PRM approach. All actual calculations are performed as described in Ref. [4], and the half-filled HM is only considered in the one-dimensional case.

Adiabatic Limit. In the following we discuss the results for the one-phonon and one-electron spectral functions, $B(q; \omega)$, $A_k^+(\omega)$, and $A_k^-(\omega)$. We start with the adiabatic limit ($\epsilon_0 = t$) where the metallic as well as the insulating phase can be described within the PRM approach. In panel (a) of Fig. 1, $A_k^+(\omega)$ and $A_k^-(\omega)$ are shown for different values of the wave vector k as functions of ω . The used parameters, $\epsilon_0 = 0.4t$, $g = 0.632t$, belong to the metallic region in the adiabatic limit so that no gap occurs at the Fermi level at $\epsilon = 0$. Both functions are dominated by the coherent electronic excitation at ϵ_k [8]. We also find incoherent excitations distributed over an energy range of about $2\epsilon_0$.

As one can see in panel (b) of Fig. 1, the frequency behavior of the phonon spectral function $B(q; \omega)$ is also dominated by the coherent excitation at ϵ_q [8] in this parameter regime. If the EP coupling g is close to the critical value g_c of the metal-insulator transition, a strong softening of the coherent excitation at ϵ_q can be observed in the adiabatic limit for q values approaching the Brillouin zone boundary at $q = \pi$. This phonon softening is caused by the coupling to electrons and has already been discussed in Refs. [4, 7]. It will turn out that a phonon hardening occurs in the anti-adiabatic limit.

Panel (b) of Fig. 1 shows that the energies of the incoherent excitations are distributed over an energy range of the order of the electronic bandwidth. According to Eq. (5), the energy spreading is caused by the energy differences of electronic particle-hole excitations $(\epsilon_{k+q} - \epsilon_k)$ where k runs over the whole Brillouin zone. From the numerator in Eq. (5), $[f(\epsilon_k) - f(\epsilon_{k+q})]$,

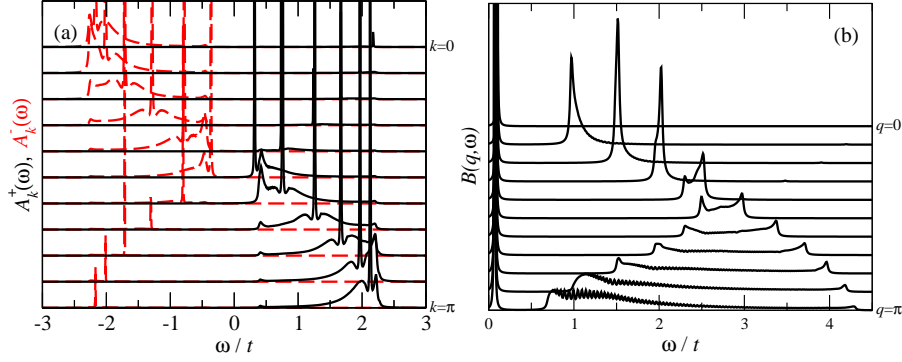


Fig. 2 { (Color online) As Fig. 1 but for $\beta_0 = 0.1t$, $g = 0.3t$ (adiabatic case, insulating phase).

one concludes that either ϵ_k is smaller and ϵ_{k+q} larger than the Fermi energy or vice versa. In agreement with Fig. 1, Eq. (5) also shows that the energy range of the incoherent excitations increases with increasing q . Due to the absence of an electronic gap in the metallic phase, incoherent excitations with small energies are present for q -values close to $q = 0$ and $q = \pi$.

Next, let us consider the ordered insulating phase in the adiabatic limit, $\beta_0 = t^{-1}$, where $\beta_0 = 0.1t$ and $g = 0.34t$ have been chosen. The gap of order $\sim 0.37t$ in the electronic excitation spectrum [compare panel (a) of Fig. 2] clearly shows that the system is in the insulating state. Again the electronic spectral functions $A_k^+(\omega)$ and $A_k^-(\omega)$ are dominated by the coherent excitation at ϵ_k , and the spreading of the incoherent excitations is similar to that of the metallic state [compare with panel (a) of Fig. 1]. As one can see in panel (b) of Fig. 2, the spectral weight of the coherent excitation is for the phonon spectral function $B(q, \omega)$ again huge in comparison to that of the incoherent excitations. However, it is important to notice a significant difference to the metallic state [compare panel (b) of Fig. 1]: No incoherent excitations occur at low energies which corresponds to the gap in the electronic spectrum.

Anti-adiabatic Limit. Next we discuss the anti-adiabatic limit where $\beta_0 = t^{-1}$ holds. Unfortunately, in this limit we are restricted to the metallic case $g < g_c$, because no stable solution for the insulating phase $g > g_c$ is found within the PRM approach. The reason is that the absolute value of the EP coupling g is too large in this case. As one can see in Ref. [4], the renormalization equations were derived by starting from an uncorrelated model by successively eliminating high-energy excitations which prevents the application of the PRM scheme for extremely high coupling parameters g . The electronic spectral functions $A_k^+(\omega)$ and $A_k^-(\omega)$ are shown in panel (a) of Fig. 3 for the metallic phase, where $\beta_0 = 4t$ and $g = 2.82t$ have been chosen. The missing gap in the electronic spectrum reveals the metallic state of the system, and the k dependence of the sharp coherent excitation peak corresponds to the dispersion ϵ_k of the electrons. The coherent excitation is separated from the incoherent excitations by an energy of the order of the phonon energy β_0 . Here, a renormalized one-electron creation operator c_k^γ has been used which includes phonon operators only in linear order (see Ref. [7] for details). This coupling leads to the energetic separation of order β_0 . If operator terms with more than a single phonon operator were taken into account additional excitations at higher frequencies ($2\beta_0$, $3\beta_0$, etc.) would appear. This is confirmed by recent ED results of [9].

The metal-insulator transition in the anti-adiabatic limit can be understood as the formation of small immobile polarons which are electrons surrounded by clouds of phonon ex-

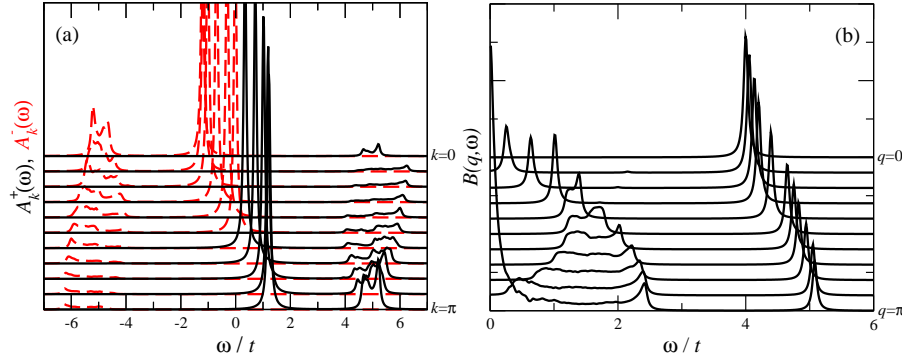


Fig. 3 (Color online) As Fig. 1 but for $\epsilon_0 = 4t$, $g = 2.82t$ (anti-adiabatic case, metallic phase).

citations. In the PRM approach polarons correspond with the fully renormalized electronic excitations μ_k . If one compares the renormalized electronic band width for the adiabatic case, which can be read off from the coherent excitation in panel (a) of Fig. 1, with that of Fig. 3 in the anti-adiabatic case one observes a strong reduction of the band width. This reduction clearly indicates localization tendencies in the system which might allow the determination of the critical EP coupling g_c of the metal-insulator transition in the anti-adiabatic limit within our PRM approach [10].

Panel (b) of Fig. 3 shows the phononic spectral function $B(q; \omega)$ in the anti-adiabatic limit. It is important to notice three significant differences to the adiabatic case [compare with panel (b) of Fig. 1]: Firstly, the coherent phonon excitation no longer shows a softening behavior, instead an hardening of the phonon modes is observed from a value ϵ_0 at $q = 0$ to higher energies for all $q > 0$. Secondly, the incoherent contributions from particle-hole excitations have gained considerable weight as compared to the adiabatic case [see panel (b) of Fig. 1]. The energy range of the incoherent excitations is again of the order of the electronic band width. Finally, a huge elastic contribution is found in $B(q; \omega)$ for $q = 0$.

Discussion. Phononic and electronic spectral functions for the one-dimensional HM at half-filling were recently evaluated in Ref. [9]. In this work, the same parameter values as used here were studied by exact diagonalization techniques (ED) for system sizes of up to 10 lattice sites. The results for the electronic spectral functions $A_k^+(\omega)$ and $A_k^-(\omega)$ agree quite well with our analytical results in the whole metallic regime. In the phonon spectrum two essential differences are found. In the ED-approach [9] a strong excitation is found at frequency $\omega = 0$ for wave vector $q = 0$ both in the adiabatic and in the anti-adiabatic case. In contrast, the results in Figs. 1 and 3 show excitations for small q only for finite frequencies $\omega > 0$. This additional zero-frequency peak in Ref. [9] is caused by a different definition of the phonon spectral function. Instead of the commutator spectral function $B(q; \omega)$, in [9] a phononic correlation function, $B'(q; \omega) = \frac{1}{2} \text{Re} \int_0^\infty dt e^{i\omega t} \langle [b_q(t), b_q^\dagger(0)] \rangle$, is investigated so that an additional zero-frequency contribution from the center of gravity motion contributes, which is dropped in the commutator spectral function as defined in Eq. (3).

The second difference between our results and those of the ED approach of Ref. [9] is more important: In the phonon spectrum of [9] almost no small frequency excitations are found in the vicinity of $q = \pi$ whereas the present PRM approach for $B(q = \pi; \omega)$ in the anti-adiabatic limit gives a strong zero-energy peak at $q = \pi$. For a more detailed discussion let us consider the phonon spectrum for different q -values in the vicinity of $q = \pi$ [panel (b) of Fig. 4].

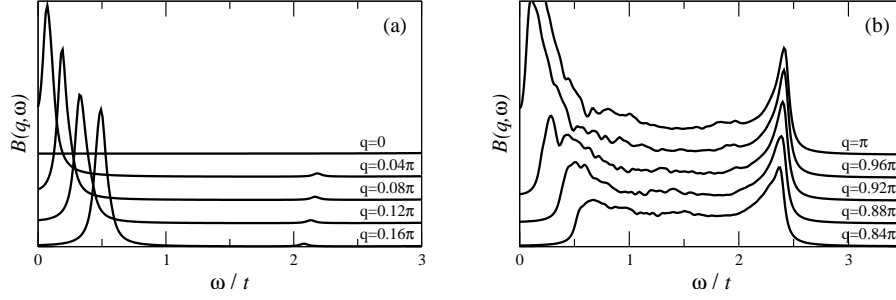


Fig. 4 { Low energy range of the phonon spectral function as shown in Fig. 3 for small q values [panel (a)] and for q values close to the Brillouin-zone boundary [panel (b)].

As follows from (5), the incoherent excitations in $B(q; \omega)$ are caused by the coupling of the phonons to electronic particle-hole excitations with energies $\epsilon_{k+q} - \epsilon_k$ where the wave vector k runs over the whole Brillouin zone. The energies ϵ_{k+q} and ϵ_k have to be below and above the Fermi level with momentum k_F . Thus, only electronic particle-hole excitations contribute with either $k < k_F$ and $k+q > k_F$, or $k > k_F$ and $k+q < k_F$. For $q=0$ this condition is fulfilled for all k -values of the Brillouin zone, and incoherent excitations are found in an energy regime of the order of the electronic band width. For $q=0$ the smallest possible energy difference $\epsilon_{k+q} - \epsilon_k$ is the same as the energy difference of two neighboring k points around k_F with the smallest possible distance in k -space. This distance is of order $1/N$ and might be not small for a small system size. This explains the absence of low-energy excitations in the phonon spectrum of Ref. [9] close to the Brillouin-zone boundary (where only system sizes of order $N=10$ have been considered). We could confirm this mechanism within our PRM approach: If we reduce the system size from 500 to 66 lattice sites the low-frequency peak in $B(q=0; \omega)$ is almost completely suppressed, and its position is shifted to higher energies.

Let us also discuss the case of small q -values $q \ll \pi$, where only k values from the sum in (5) can contribute which are located in a small wave vector region around the Fermi momentum k_F . Assuming a linear momentum dependence for energies close to Fermi energy, the incoherent electronic excitation energies can be replaced by $\epsilon_{k+q} - \epsilon_k \approx v_F q$. (v_F is the Fermi velocity.) For small q the position of the incoherent excitations is proportional to q , as seen in panel (a) of Fig. 4. On the same time the intensity of the incoherent peak is approximately q independent which follows again from (5): The linear q dependence of the denominator is canceled by the number of contributing k points which is also proportional to q so that an approximately q independent intensity results.

Finally, we use the PRM to evaluate the Luttinger liquid parameters u, K in the metallic phase at half-filling. It is commonly accepted that the spinless one-dimensional HM belongs to the Tomonaga-Luttinger universality class, and at $T=0$ a Luttinger liquid should be realized. Due to the quite different behavior of the phonon spectral function in the adiabatic and in the anti-adiabatic regime one expects different results in both cases. For the velocity u of the charge excitations, we use a finite-size scaling of the energy gap [11,12],

$$\Delta = \frac{1}{2} (E_0^{+1} + E_0^{-1} - 2E_0) = \frac{u}{N} \frac{1}{2},$$
 where N is the lattice size, and E_0 denotes the ground-state energy of the half-filled system. $E_0^{\pm 1}$ is the ground-state energy of the system with ± 1 fermions away from half-filling. To compute the effective coupling constant K we take the first derivative of the charge correlation function $C(q)$ at $q=0$, $\frac{\partial C(q)}{\partial q} \Big|_{q=0} = \frac{K}{u}$, where
$$C(q) = \frac{1}{N} \sum_{i,j} e^{iq(R_i - R_j)} \langle n_i n_j \rangle.$$
 Results are given in Table I. In the anti-adiabatic

	$t_0 = t = 0.1$			$t_0 = t = 4.0$		
$g=t$	0.078	0.141	0.2	1.0	1.8	2.82
K	0.966	0.888	0.882	0.928	0.790	0.740
$u = 8t$	0.978	0.933	0.928	0.935	0.708	0.647

Table I: LL parameters in the adiabatic and in the anti-adiabatic regime. To account for the missing spin degree of freedom, K has been multiplied by a factor of 2.

regime the parameter u for the kinetic energy is strongly reduced when g is increased which corresponds to the band width reduction as discussed above [compare panel (a) of Fig. 3]. This behavior of u is very similar to recently found results [13]. In contrast, the results for K represent an unsolved puzzle: Here, K is always smaller than 1, whereas in Ref. [13] K was smaller than 1 only in the anti-adiabatic regime but larger than 1 in the adiabatic regime.

Summary. { In this paper we have considered the phononic and electronic spectral functions of the one-dimensional HM at filling. In particular, we have studied the spectral signatures of the metallic phase both in the adiabatic and the anti-adiabatic limit, and of the insulating phase in the adiabatic limit. (The insulating state could not be investigated in the anti-adiabatic limit because the employed PRM approach breaks down in this case.) We find a quite strong coupling of the phonon dynamics to electronic particle-hole excitation which leads to incoherent contributions to the phononic spectral function. In particular, a dominant incoherent low-energy peak is observed for the metallic phase in the anti-adiabatic limit.

We would like to acknowledge helpful discussions with H. Fehske. This work was supported by the DFG through the research program SFB 463.

REFERENCES

- [1] Bishop A.R. and Swanson B.I., Los Alamos Science, 21 (1993) 133; Tsuchida N. et al., Electronic Conduction in Oxides (Springer-Verlag, Berlin) 1990;
- [2] Farges J.-P. (Editor), Organic Conductors (Marcel Dekker, New York) 1994.
- [3] Lanzara A. et al., Nature, 412 (2001) 510; Millis A.J., Littlewood P.B., and Shraiman B.I., Phys. Rev. Lett., 74 (1995) 5144; Gunnarson O., Rev. Mod. Phys., 69 (1997) 575.
- [4] Sykora S., Hubsch A., and Becker K.W., Eur. Phys. J. B, 51 (2006) 181.
- [5] Fehske H., Holicki M., and Weie, A. in Advances in Solid State Physics, Vol. 40, edited by Kramer B. (Vieweg, Wiesbaden) 2000, p. 235.
- [6] Becker K.W., Hubsch A., and Sommer T., Phys. Rev. B, 66 (2002) 235115.
- [7] Sykora S. et al., Phys. Rev. B, 71 (2005) 045112.
- [8] Here we suppressed the band index for the one-particle energy because it is not needed for metallic solutions. See Ref. [4] for details.
- [9] Hohenadler M. et al., Phys. Rev. B, 73 (2006) 245120.
- [10] Sykora S., Hubsch A., and Becker K.W., to be published.
- [11] Schulz, H.J., Int. J. Mod. Phys. B, 5 (1991) 57.
- [12] S. Daul and R.M. Noack, Phys. Rev. B, 58 (1998) 2635.
- [13] H. Fehske et al., Physica B, 359-361 (2005) 699.